Short communication

# Oxygen reduction at carbon supported ruthenium–selenium catalysts: Selenium as promoter and stabilizer of catalytic activity

Hendrik Schulenburg [a,*], Marcus Hilgendorff [a], Iris Dorbandt [a], Jörg Radnik [b],
Peter Bogdanoff [a], Sebastian Fiechter [a], Michael Bron [a], Helmut Tributsch [a]

[a] *Hahn-Meitner-Institut Berlin, Abteilung Solarenergieforschung 5, Glienicker Strasse 100, D-14109 Berlin, Germany*
[b] *Institut für Angewandte Chemie Berlin-Adlershof, Richard-Willstätter Strasse 12, D-12489 Berlin, Germany*

## Abstract

Carbon supported ruthenium-based catalysts (Ru/C) for the oxygen reduction in acid electrolytes were investigated. A treatment of Ru/C catalysts with selenious acid had a beneficial effect on catalytic activity but no influence on intrinsic kinetic properties, like Tafel slope and hydrogen peroxide generation. Reasons for the increased activity of $RuSe_x/C$ catalysts are discussed. Potential step measurements suggest that at potentials around 0.8 V (NHE) a selenium or selenium-oxygen species protects the catalyst from formation of inactive $RuO_2$-films. This protective effect leads to an enhanced activity of $RuSe_x/C$ compared to Ru/C. No evidence was found for a catalytically active stoichiometric selenium compound. The active phase may be described as a ruthenium suboxide $RuO_x$ ($x < 2$) layer integrated in a $RuSe_y$ phase or $RuSe_yO_v$ ($y < 2$, $v < 2$) layer at the particle surface.
© 2005 Published by Elsevier B.V.

*Keywords:* Oxygen reduction; Ruthenium; Selenium; $RuO_2$; Anodic stability

## 1. Introduction

Direct methanol fuel cells (DMFCs) are discussed as portable power sources for electronic devices, such as laptops, cellular phones or video cameras. Due to their high catalytic activity carbon supported platinum nanoparticles are used as catalyst for the oxygen reduction in DMFCs [1–3] However, the high price and poor selectivity of platinum in the presence of methanol [4–6] motivated the search for alternative cathode catalysts. Ruthenium–selenium catalysts are a promising alternative because they show excellent selectivity for oxygen reduction in presence of methanol [7] and are also much cheaper than platinum. One way to

prepare ruthenium–selenium catalysts is by thermolysis of $Ru_3(CO)_{12}$ in selenium saturated organic solvents [8–12]. Active catalysts can also be obtained without selenium, but the addition of selenium improves the activity and stability of the catalysts significantly. The beneficial effect of selenium is somewhat surprising since chalcogens are usually known as poison for metal catalysts. As an explanation for this effect Bron et al. [10,11] and Tributsch et al. [12] proposed that the catalysts consists of surface modified ruthenium nanoparticles when prepared with $Ru_3(CO)_{12}$ as educt. The formation of the catalytically active centers should be facilitated by selenium, however, the exact structure of this surface modification has not been identified. In contrast to this explanation, Le Rhun [13] proposed that a new catalytically active compound with the formula $RuSe_x$ was formed.

In this work, the effect of selenium on ruthenium–selenium catalysts which were prepared via a new colloidal route using $RuCl_3 \cdot xH_2O$ as precursor [14] is investigated and discussed. These catalysts show higher ruthenium dispersion

* Corresponding author at: Max-Planck-Institut für Kohlenforschung, AK Reetz, Kaiser-Wilhelm-Platz 1, 45470 Mülheim an der Ruhr, Germany. Tel.: +49 208 306 2393; fax: +49 208 306 2985.

*E-mail address:* schulenburg@mpi-muelheim.mpg.de (H. Schulenburg).

and higher activities than catalysts prepared by thermolysis of $Ru_3(CO)_{12}$. Ru/C and $RuSe_x$/C catalysts with different quantities of selenium were prepared and investigated by rotating (ring) disc electrode method (R(R)DE), X-ray photoelectron spectroscopy (XPS), neutron activation analysis (NAA) and potential step techniques. Reasons for the beneficial effect of selenium on the catalytic activity for oxygen reduction are discussed.

## 2. Experimental

### 2.1. Catalyst preparation

The catalyst preparation was described by Hilgendorff [14]. An amount of 2.8 g $RuCl_3$ were dissolved in 500 ml tetrahydrofuran (THF). An amount of 100 ml of a 0.4 M solution of $N(C_8H_{17})BEt_3H$ in THF were added drop by drop, followed by the addition of 100 ml ethanol. The solution was centrifuged at 4500 rpm for 15 min. The residue was washed with ethanol twice and dried in an argon atmosphere. An amount of 0.35 g of thus obtained powder was dissolved in 250 ml THF. Under vigorous stirring this solution was added to a suspension of 0.85 g carbon black (Vulcan XC72) in 250 ml THF. The solvent was removed under reduced pressure and the residue was washed with $H_2O$/ethanol (10/90 vol.%). The dried powder was exposed to a hydrogen atmosphere at 300 °C and washed again with ethanol (p.A.). The resulting Ru/C catalyst had a metal loading of 20%. For preparation of ruthenium–selenium catalysts, 1 g Ru/C catalyst was transferred into a solution of selenious acid in water (Table 1). The suspensions were treated in an ultrasonic bath for 15 min. After filtration, the dried powder was heated at 300 °C in a hydrogen atmosphere. The resulting catalyst is labeled $RuSe_x$/C.

### 2.2. Electrochemical characterization (RDE, RRDE)

Rotating disc electrode (RDE) and rotating ring disc electrode (RRDE) measurements were performed with Ru/C and $RuSe_x$/C catalysts. Measurements were carried out at room temperature in a three electrode arrangement, one compartment cell. Oxygen or nitrogen saturated 0.5 M $H_2SO_4$ was used as electrolyte. The counter electrode was a platinum foil, a mercury/mercury sulfate electrode (+650 mV versus normal hydrogen electrode (NHE)) served as reference. To prepare working electrodes mirror-polished Glassy Carbon disc electrodes (3 mm diameter) were used as substrate for the catalysts. The catalysts were attached to the Glassy Carbon disc in the following way: 1 mg catalyst per 100 μl de-ionized water and 100 μl of an ethanolic Nafion solution (0.2% Nafion) were ultrasonically dispersed for 15 min. A 5 μl aliquot of the suspension was dropped onto the Glassy Carbon electrode and the suspension was air-dried at room temperature.

RRDE measurements were performed with the same working, reference and counter electrode as the RDE experiments. The ring electrode was made of platinum. The radius of the disc electrode was 1.5 mm, the inner and outer radii of the ring electrode 2.3 and 5.2 mm, respectively. A theoretical collection efficiency of 0.634 was calculated with the formula given by Albery and Hitchman [15]. The collection efficiency was also determined experimentally. For that purpose, the catalyst was attached to the disc electrode and the collection efficiency was determined with the $Fe^{2+/3+}$ redox couple. The experimental collection efficiency was 0.63. For the detection of $H_2O_2$, a ring potential of 1.4 V (NHE) was applied. All polarization curves were performed as cathodic going sweeps in the range from 0.85 to 0.0 V (NHE) at a scan rate of 5 mV s$^{-1}$.

### 2.3. XPS

XP-spectra were recorded employing a Fisions ESCALAB220 iXL spectrometer working with a monochromatic Al Kα X-ray source. The samples were fixed with a double sticking C-tape to the sample holder and measured with a 150 μm spot to avoid an influence of the C-tape on the spectra. The spectra were deconvoluted with mixed Gauss–Lorentzian curves.

## 3. Results

### 3.1. Electrochemical characterization

The catalytic activity of Ru/C and $RuSe_x$/C catalysts was calculated from RDE–polarization curves (Fig. 1) using the Levich–Koutecky Eq. (1):

$$\frac{1}{i} = \frac{1}{i_{kin}} + \frac{1}{i_{dif}} = \frac{1}{i_{kin}} + \frac{1}{B\omega^{1/2}} \quad (1)$$

where $i$ is the current density, $i_{kin}$ the kinetic current density, $i_{dif}$ the diffusion limited current density and $\omega$ is the rotation rate. The kinetic current density is proportional to the activity of the catalysts. The constant $B$ is $0.62nFcD^{2/3}\nu^{-1/6}$, where $c$ is the bulk concentration of oxygen ($c = 1.1 \times 10^{-6}$ mol cm$^{-3}$), $D$ the diffusion constant of oxygen ($D = 1.8 \times 10^{-5}$ cm$^2$ s$^{-1}$) and $\nu$ is the kinematic viscosity of the electrolyte ($\nu = 10^{-1}$ cm$^{-2}$ s$^{-1}$). Increasing con-

Table 1
Effect of $H_2SeO_3$ treatment on selenium content and catalytic activity of $RuSe_x$/C catalysts

| $H_2SeO_3$ concentration (mol l$^{-1}$) | Selenium content in catalyst (%)[a] | Catalytic activity at 0.7 V (NHE) (mA cm$^{-2}$)[b] |
|---|---|---|
| 0 | 0 | 0.5 |
| $6 \times 10^{-5}$ | 0.14 | 1.6 |
| $6 \times 10^{-4}$ | 0.63 | 2.4 |
| $6 \times 10^{-3}$ | 1.23 | 3.1 |
| $6 \times 10^{-2}$ | 4.52 | 2.2 |

[a] Determined by neutron activation analysis.
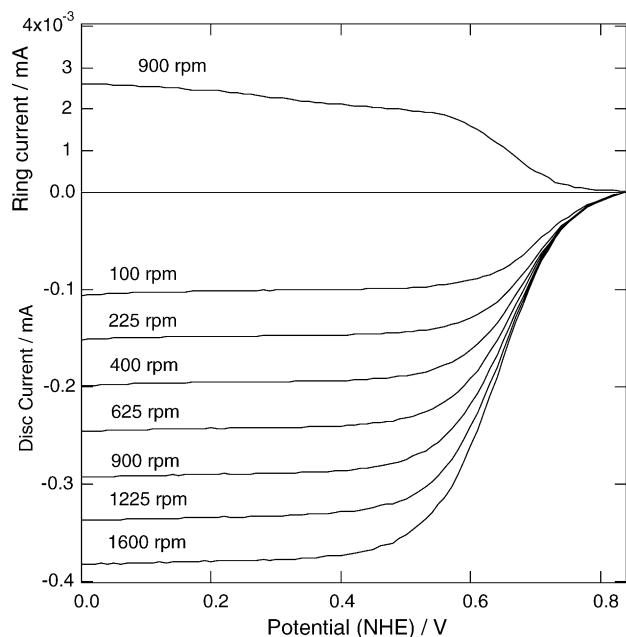[b] Calculated from RDE data, 20% metal loading, 70 μg Ru cm$^{-2}$.

Fig. 1. RRDE polarization curves of RuSe$_x$/C (0.14% Se, 20% metal loading); 70 µg Ru cm$^{-2}$; sweep rate, 5 mV s$^{-1}$; ring potential, 1.4 V (NHE). Electrolyte is oxygen saturated 0.5 M sulfuric acid.

centrations of selenium in the catalysts lead to higher catalytic activities (Table 1). Only for the highest concentration of selenious acid (60 mmol l$^{-1}$), the activity decreases. The Tafel slope is almost independent of the H$_2$SeO$_3$ treatment (Fig. 2). This suggests that the rate determining step of the oxygen reduction remains unchanged. Rotating disc electrode measurements show that the activity of Ru/C and RuSe$_x$/C catalysts is almost unchanged when 0.5 M methanol is added to the electrolyte. Both types of catalysts are therefore selective towards the oxygen reduction and are also not poisoned by methanol.

The hydrogen peroxide generation of both catalysts was estimated with the ring disc technique using Eq. (2) [16]:

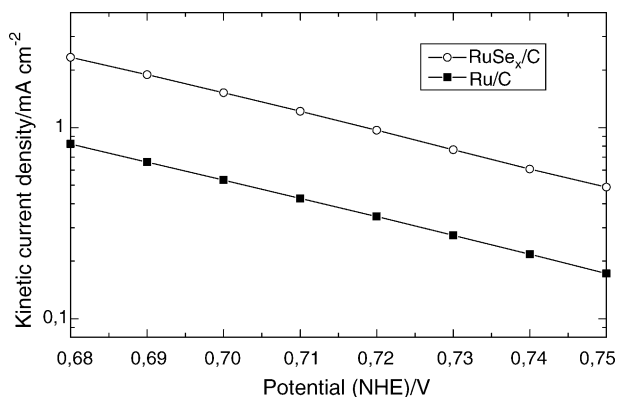$$H_2O_2(\%) = \frac{200 \frac{I_r}{N}}{\frac{I_r}{N} + |I_d|} \tag{2}$$



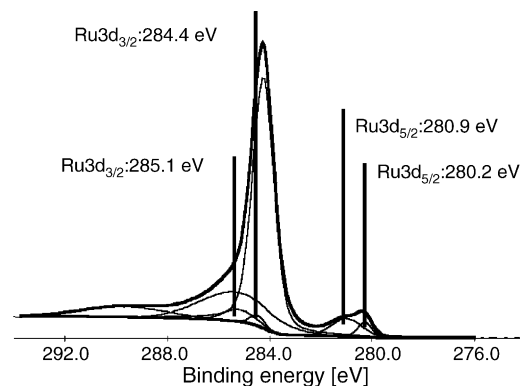Fig. 2. Tafel curves for RuSe$_x$/C (0.14% Se) and Ru/C catalysts calculated from RDE data in Fig. 1.



Fig. 3. Ruthenium 3d spectrum of RuSe$_x$/C (0.14% Se) catalyst.

with the ring current $I_r$, the disc current $I_d$ and the collection efficiency $N$. Eq. (2) was derived for a parallel mechanism where oxygen is reduced to water and hydrogen peroxide. Within the error range both catalysts generate the same amount H$_2$O$_2$, about 3% at 0.7 V (NHE).

### 3.2. XPS

The Ru 3d$_{5/2}$ spectrum of RuSe$_x$/C (Fig. 3) can be deconvoluted with two subspectra. The first has a binding energy of 280.2 eV. This component can be assigned to metallic ruthenium (binding energy 280.0 eV [17]). The binding energy of the second peak is 280.9 eV which is very similar to the Ru 3d$_{5/2}$ binding energy of RuO$_2$ (binding energy 280.7 eV [17]). Selenium is observed in two different forms with Se 3d$_{5/2}$ binding energies of 58.3 and 54.8 eV (Fig. 4). Selenium in a high oxidation state like adsorbed H$_2$SeO$_3$ or SeO$_3^{2-}$ [18] causes the first peak (58.3 eV). The second peak (54.8 eV) is more difficult to assign. Binding energies from 54.6 to 55.0 eV [19] were reported for elemental selenium, but also RuSe$_2$ has a similar binding energy (54.6 eV [20]). The Se 3d spectra suggest that during the reduction of the catalyst by hydrogen only a part of the adsorbed selenious acid is reduced to elemental selenium or a selenide. The other part obviously remains in a high oxidation state or is reoxidized after exposure to air.
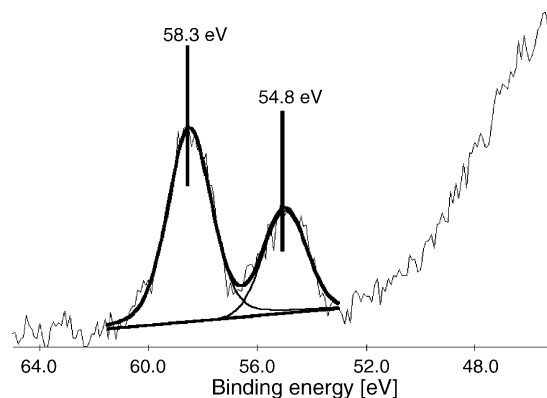


Fig. 4. Selenium 3d spectrum of RuSe$_x$/C (0.14% Se) catalyst.

## 4. Discussion

The increased activity of RuSe$_x$/C compared to Ru/C is significant. The kinetic current density at 0.7 V (NHE) is up to six times higher after Ru/C was treated in aqueous solutions of selenious acid and subsequently reduced by hydrogen (Table 1). A different particle size cannot explain this effect since TEM measurements [14] have shown that the particle size of both catalysts is 2.5 nm. A formation of an active RuSe$_x$ phase was proposed as explanation for the increased activity of catalysts which were prepared by thermolysis of Ru$_3$(CO)$_{12}$ [13]. XPS measurements of RuSe$_x$/C catalysts prepared by the Hilgendorff route [14](Fig. 4) point to the presence of H$_2$SeO$_3$ or SeO$_3^{2-}$ (binding energy, 58.3 eV) and zerovalent selenium or RuSe$_2$ (binding energy, 54.8 eV). However, own experiments show that nanocrystalline RuSe$_2$ is almost inactive for the oxygen reduction reaction. Catalytic activity of other selenium or ruthenium selenium species (Se$^0$, H$_2$SeO$_3$, ruthenium selenates) was also never reported. A comparision of the catalytic properties of Ru/C and RuSe$_x$/C catalysts (Table 2) shows that all intrinsic kinetic properties are the same: Tafel slope, hydrogen peroxide generation, selectivity in presence of methanol as well as inertness against methanol poisoning. This is strong evidence that active sites of both types of catalysts are essentially the same. Since the Tafel slope is not changed, but the catalytic activity is, the treatment with selenious acid influences the exchange current density. A higher exchange current density of RuSe$_x$/C catalysts can be explained with a larger rate constant for the oxygen reduction at the equilibrium potential or just by an enlarged effectively acting catalytic area. The catalytically active area can be influenced by the in situ oxide coverage of the catalysts, since ruthenium electrodes form different surface oxides RuO$_x$, with $0 < x < 4$, whereby the oxidation state depends on the applied potential [21–24]. According to ellipsometric studies of Velikodny [24] between 0 and 0.7 V (NHE), a surface oxide RuO$_x$ with $0 < x < 1$ is present. In the range from 0.7 to 0.9 V (NHE) $x$ varies between 1 and 2, in this potential region the formation of RuO$_2$ starts. At even higher potentials the electrode surface is oxidized completely to RuO$_2$. Higher ruthenium oxides are only generated at potentials which are not relevant for the oxygen reduction. RuO$_2$ films show a poor activity for

the oxygen reduction due to the specific electronic structure of the semimetallic material, therefore, ruthenium catalysts should not be exposed to potentials which are higher than about 0.85 V(NHE), otherwise they become inactivated by the formation of RuO$_2$ films. These films can be reduced if the electrode is exposed to these high potentials only for a short time, but the electrochemical reduction of thick RuO$_2$ films is very slow or even impossible [25]. In contratst the activity of ruthenium–selenium catalysts is less affected by anodic polarization. This could point to a lower degree of oxidation of ruthenium in presence of selenium. In order to investigate the in situ oxide formation of Ru/C and RuSe$_x$/C, potential step experiments were performed (Fig. 5).

At first, the catalysts are reduced at a potential of 0.05 V (NHE). At this potential, the oxidation state of ruthenium is almost zero. Then, a potential step to more positive potentials is applied and the anodic charge is measured as function of the polarization time. The potential steps last 1–100 s. On that time scale, the charge originates mainly from oxide formation. Fig. 5 shows that charges for Ru/C are significantly higher than for RuSe$_x$/C. This is observed for all investigated potentials. Selenium treated catalysts are more resistant against oxidation. It is also remarkable that the plot of anodic charge against logarithmic polarization time is only linear for Ru/C. A linear course is expected for the formation of surface oxides [23,25,26]. The anodic charge and therefore the in situ oxidation of RuSe$_x$/C is much lower. Concerning the RuSe$_x$/C catalyst, the charge increases also with the step time and more positive potentials. An oxide film is formed described with the general formula RuO$_x$. More positive potentials and longer step times lead to higher values for $x$ in RuO$_x$. But

**Table 2**
Kinetic properties of Ru/C and RuSe$_x$/C catalysts

| | Ru/C | RuSe$_x$/C (0.14% Se) |
|---|---|---|
| Tafel slope | $105 \pm 4$ mV dec$^{-1}$ | $109 \pm 2$ mV dec$^{-1}$ |
| H$_2$O$_2$ generation at 0.7 V (NHE) | $3 \pm 1$% | $3 \pm 1$% |
| Selective oxygen reduction in presence of methanol | Yes | Yes |
| Poisoned by methanol | No | No |
| Catalytic activity at 0.7 V (NHE) (mA cm$^{-2}$)[a] | 0.5 | 1.6 |

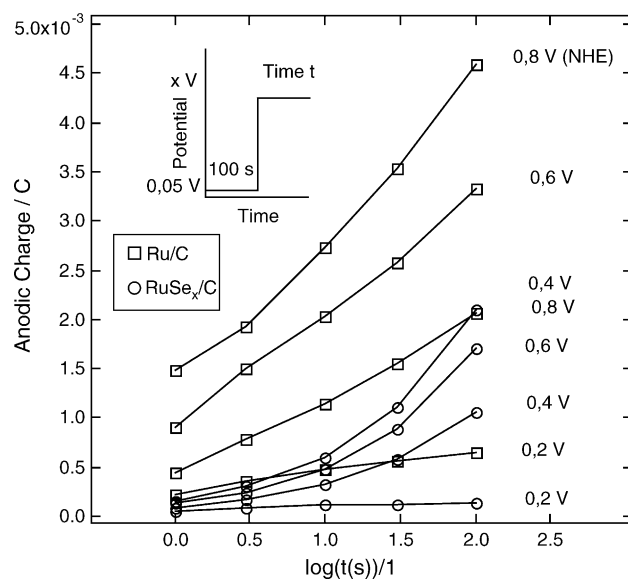[a] Calculated from RDE data, 20% metal loading, 70 $\mu$g Ru cm$^{-2}$.



Fig. 5. Plot of anodic charge vs. logarithmic potential step time. RuSe$_x$/C (0.14% Se) and Ru/C catalysts were reduced for 100 s at 0.05 V (NHE) and an anodic potential step (inset) is applied for $t = 1(3, 10, 30, 100)$ s. The anodic charge is calculated from integrating current vs. step time plots. The potential is stepped from 0.05 (NHE) to 0.2(0.4; 0.6; 0.8) V (NHE). Electrolyte was nitrogen saturated 0.5 M sulfuric acid.

for any potentials and step times, the degree of oxidation is much lower for the $RuSe_x$/C catalyst, especially at potentials between 0.4 and 0.8 V (NHE). This suggests that the improved activity of $RuSe_x$/C is not due to formation of an active selenium compound, but it is caused by stabilization of the catalytically active surface area against oxidation. In the potential region around 0.8 V (NHE) less inactive $RuO_2$ is formed therefore more active sites are available. Selenium or selenium-oxygen species will bind on $RuO_x$ ($x < 2$) nanoparticles during the preparation of $RuSe_x$/C catalysts. An inhibition of oxidation may be caused by occupation of favored electro-crystallization sites of $RuO_x$ ($x < 2$) or by an increased electron density in the $RuO_x$ ($x < 2$) nanoparticles due to electron transfer from the selenium species. Only an overpotential can overcome this inhibition, which is shown by potential step experiments (Fig. 5). Further evidence for this interpretation comes from EXAFS measurements (Fiechter et al., in preparation) which show Ru–Se distances. To sum up, in $RuSe_x$/C catalysts selenium or selenium-oxide species are bonded to $RuO_x$ nanoparticles. These selenium species lead to a conservation of more $RuO_x$ ($x < 2$) sites under in situ conditions. This leads to a higher catalytic activity compared to $RuO_x$/C catalysts. This explanation for the increased activity of $RuSe_x$/C compared to Ru/C is in agreement with the kinetic results (Figs. 1 and 2), because the active sites are in both cases the same and essentially based on the Ru-centers. But at potentials around 0.8 V (NHE) more active sites are available at the $RuSe_x$/C catalyst.

## 5. Conclusion

The improved activity towards the oxygen reduction reaction of $RuSe_x$/C catalysts compared to Ru/C catalysts was explained by different in situ oxide coverage. A selenium compound itself is not catalytically active in $RuSe_x$/C, but selenium or a selenium-oxygen species is able to suppress the formation of inactive $RuO_2$ in the potential region around 0.8 V (NHE). This effect leads to a larger catalytically active area compared to Ru/C and therefore to higher activity and improved anodic stability.

## Acknowledgements

## References

[1] L. Carrette, K.A. Friedrich, U. Stimming, ChemPhysChem 1 (2000) 162.
[2] E. Antolini, Mater. Chem. Phys. 78 (2003) 563.
[3] S.C. Thomas, X.M. Ren, S. Gottesfeld, P. Zelenay, Electrochim. Acta 47 (2002) 3741.
[4] A. Heinzel, V.M. Barragan, J. Power Sources 84 (1999) 70.
[5] M.K. Ravikumar, A.K. Shukla, J. Electrochem. Soc. 143 (1996) 2601.
[6] J. Kallo, W. Lehnert, R. von Helmolt, J. Electrochem. Soc. 150 (2003) A765.
[7] N. Alonso-Vante, P. Bogdanoff, H. Tributsch, J. Catal. 190 (2000) 240.
[8] N. Alonso-Vante, H. Tributsch, O. Solorza-Feria, Electrochim. Acta 40 (1995) 567.
[9] N. Alonso-Vante, M. Gersig, H. Tributsch, J. Electrochem. Soc. 138 (1991) 639;
V. Trapp, P. Christensen, A. Hamnett, J. Chem. Soc. 92 (1996) 4311.
[10] M. Bron, P. Bogdanoff, S. Fiechter, I. Dorbandt, M. Hilgendorff, H. Schulenburg, H. Tributsch, J. Electroanal. Chem. 500 (2001) 510.
[11] M. Bron, P. Bogdanoff, S. Fiechter, M. Hilgendorff, J. Radnik, I. Dorbandt, H. Schulenburg, H. Tributsch, J. Electroanal. Chem. 517 (2001) 85.
[12] H. Tributsch, M. Bron, M. Hilgendorff, H. Schulenburg, I. Dorbandt, V. Eyert, P. Bogdanoff, S. Fiechter, J. Appl. Electrochem. 31 (2001) 739.
[13] V. Le Rhun, N. Alonso-Vante, J. New Mater. Electrochem. Syst. 3 (2000) 331.
[14] M. Hilgendorff, K. Diesner, H. Schulenburg, P. Bogdanoff, M. Bron, S. Fiechter, J. New Mater. Electrochem. Syst. 5 (2002) 71.
[15] W.J. Albery, M.L. Hitchman, Ring-Disc Electrodes, Clarendon Press, Oxford, 1971, p. 22.
[16] U.A. Paulus, T.J. Schmidt, H.A. Gasteiger, R.J. Behm, J. Electroanal. Chem. 495 (2001) 134.
[17] D. Briggs, M.P. Seah, Practical Surface Analysis, vol. 1, Wiley, 1993.
[18] C.D. Wagner, W.M. Riggs, L.E. Davis, J.F. Moulder, Handbook of X-ray Photoelectron Spectroscopy, Perkin-Elmer Corporation, Physical Electronics Division, 1979.
[19] http://www.lasurface.com.
[20] W. Jaegermann, H-M. Kühne, Appl. Surf. Sci. 26 (1986) 1.
[21] S. Hadzi-Jordanov, H. Angerstein-Kozlowska, B.E. Conway, Electroanal. Chem. Interf. Electrochem. 60 (1975) 359.
[22] S. Hadzi-Jordanov, H. Angerstein-Kozlowska, M. Vucovic, B.E. Conway, J. Phys. Chem. 81 (1977) 2271.
[23] S. Hadzi-Jordanov, H. Angerstein-Kozlowska, M. Vucovic, B.E. Conway, J. Electrochem. Soc. 125 (1978) 1471.
[24] L.N. Velikodnyi, V.A. Sheplin, É.V. Kasatkin, Sov. Electrochem. 18 (1982) 1134.
[25] S. Trasatti, Electrodes of Conductive Metallic Oxides, Part A, Elsevier Publishing Company, 1980.
[26] K.J. Vetter, J.W. Schultze, Electroanal. Chem. Interf. Electrochem. 34 (1972) 131.